Desalination and Water Treatment
www.deswater.com

doi:10.5004/dwt.2019.24090

156 (2019) 7–19
July

Economic comparison between RO-wind and RO-PV desalination systems

Rached Ben-Mansour[a,b], A.H. Al-Jabr[a,*], R. Saidur[b,c]

[a]*Department of Mechanical Engineering, King Fahd University of Petroleum and Minerals (KFUPM), Dhahran 31261, Saudi Arabia, email: rmansour@kfupm.edu.sa (R. Ben-Mansour), aljabrah@kfupm.edu.sa (A.H. Al-Jabr)*
[b]*Center of Research Excellence in Renewable Energy (CORE-RE), King Fahd University of Petroleum and Minerals (KFUPM), Dhahran 31261, Saudi Arabia, email: saidur@sunway.edu.my (R. Saidur)*
[c]*Research Center for Nanomaterials and Energy Technology (RCNMET), School of Science and Technology, Sunway University, No. 5, Jalan University, Bandar Sunway, 47500 Petaling Jaya, Malaysia*

Received 8 November 2016; Accepted 9 March 2019

ABSTRACT

Research and development of desalination technologies are becoming highly critical because of the rapid increase in freshwater demand. Researchers are continually working on improving the existing desalination technologies and exploring new methods and ideas to desalinate salty water. The main goal is to come up with cost-effective systems. Renewable energy desalination is becoming an attractive option nowadays because of its viability of producing fresh water, technology improvement continuation, limitation of conventional sources and compatibility between water needs and renewable resources availability. More importantly, using renewable energy to power desalination systems is extremely important for reducing global emissions and protecting the environment. This research is an attempt to provide a systematic methodology for determining the most cost-effective combination of renewable energy powered reverse osmosis desalination system for a given location and required capacity. Two combinations are compared which are RO-Wind and RO-PV. Results show that for Dhahran, Saudi Arabia cost of water produced by RO-Wind is 1.366 \$/m^3 to 1.273 \$/m^3 and by RO-PV is 2.119 \$/m^3 to 2.048 \$/m^3 for a system capacity of 1000 m^3 to 10,000 m^3, respectively.

Keywords: Desalination; Renewable energy; Reverse osmosis; Wind; Photovoltaic

1. Introduction

Water is a critically important element in mankind's life. However, water demand is rapidly increasing because of the population increase and uncontrolled human and industrial usage. According to the International Desalination Association, more than 86.8 million m^3 of water is desalinated daily over the world [1]. This number is expected to increase in the near future because of the continued increase in population and industry. Research and development of desalination technologies are becoming highly significant to improve the existing technologies and exploring new techniques. The main goal is to come up with cost-effective systems.

Increasing conventional fossil fuels costs, conventional resources being depleted and its adverse environmental effects lead consumers to think in other power alternatives. On the other side, renewable energy is abundant on the earth, available, sustainable, free and environmentally friendly. Consumers are working in utilizing this energy in producing power and water. Utilization of renewable energy in purifying water is becoming more attractive nowadays. The main concern is the optimum economical selection of renewable energy powered desalination system.

Renewable Energy Desalination Systems (REDS) are categorized into direct and indirect systems. Direct REDS are stand-alone renewable desalination system such as solar stills. However, indirect REDS are systems composed of two stand-alone subsystems; renewable energy and conventional desalination, such as solar thermal-MSF, solar PV-RO, and Wind-MVC. Fig. 1 shows the possible com-

*Corresponding author.

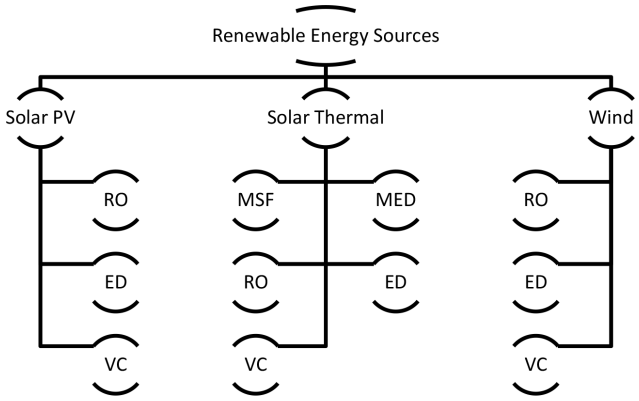

Fig. 1. Possible REDS combinations.

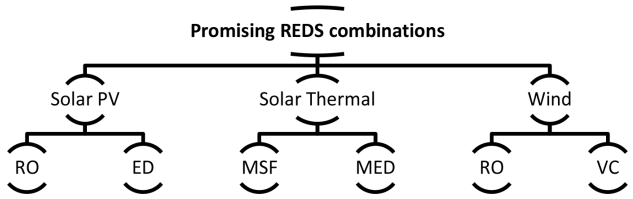

Fig. 2. Most promising REDS combinations.

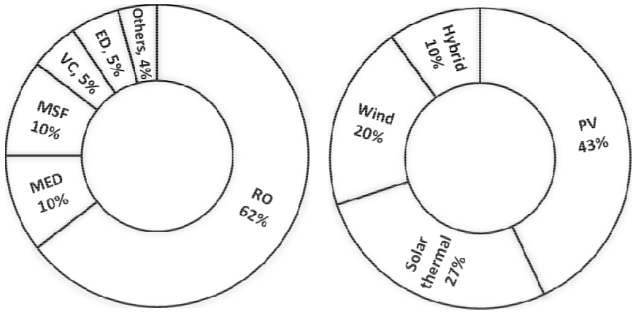

Fig. 3. Worldwide breakdown of REDS based on desalination technology (Left) and renewable energy (Right).

binations of renewable power technologies and desalination technologies. However, proper matching should be carefully investigated to end up with a rigid system that provides water at a reasonable cost. Fig. 2 shows the most promising combinations of REDS as recommended by [2]. Solar and wind energy coupled with desalination systems have been implemented and to be promising more than other renewable-desalination combinations [3]. The most renewable-desalination combinations used are PV-RO [4,5] and solar thermal-MED [5]. Fig. 3 shows the worldwide breakdown of renewable energy powered desalination capacity based on desalination technology and renewable energy, respectively.

Chauhan and Saini [6] presented a comprehensive review of integrated renewable energy systems including configuration, models, storage options and others. Kalogirou [5] reviewed industrially-proven desalination and renewable systems. Indirect solar desalination has been comprehensively reviewed by [7]. Gude et al. [3] discussed desalination systems and possible utilization of renewable energy. Authors suggested a coupling of renewable systems and reusing and recycling of water and energy. Eltawil et al. [8] indicated that the implementation of the renewable-energy powered desalination systems is slow mainly because of governmental subsidies. Evaluation of the renewable potential in the Arab regions was conducted by [2] with a brief description of desalination and renewable systems. In wind-energy powered desalination review, [9] concluded that systems coupled with wind energy are technically mature although system installation is limited. Their observation was that RO is the most utilized desalination technology powered by wind. On the other hand, the share of RO-wind is less than RO-PV.

Karagiannis and Soldatos [10] provided water desalination cost review with the conclusion that the cost of water is location dependent. A recent review of renewable energy powered desalination systems shows significant variation in the price of RO-PV and RO-Wind systems [11]. The cost of water by RO-PV is ranging from 0.825 to 34.21$/m^3 while RO-Wind is ranging from 0.66 to 15.75 $/m^3. Al-Karaghouli and Kazmerski [12] stated that desalination technologies powered by renewable energy are proven-technology and economically competitive in remote regions. Technology improvement or fossil-fuel prices rising will make these systems financially viable. Al-Karaghouli [2] presented solar-powered desalination with a capacity of less than 10 m^3/d in a remote area, where fuel, grid, and technical support are unavailable. Authors reported that only this technology is technically and economically competitive to other technologies. Ghaffour et al. [4] claimed that solar desalination cost exceeds conventional systems cost by more than four times and cannot be reduced to compete the conventional costs in the near future.

Rheinländer et al. [13] have developed a simulation tool for de-centralized supply of power and water. Power sources are renewable (wind and solar PV) and conventional (diesel). Perz and Bergmann [14] adapted the simulation tool by adding economical models for techno-economic analysis. Ahmad et al. [15] simulated photovoltaic-reverse osmosis (PVRO) system. The system was designed to operate under variable PV power due to the variable solar irradiation resulting in variable output distillate water. Simulation results were validated experimentally. They included neither other renewable and desalination systems nor cost estimation of PVRO. A comparison between four different renewable-desalination combinations has been carried by [16] for a plant capacity of 500 m^3 for a location at which average wind speed is 7.5 m/s, the average ambient temperature is 20°C, and global solar irradiation is 5 kWh/d/m^2. The results show that RO-Wind and MVC-Wind have almost the same specific cost of 1.61 and 1.62 $/ m^3, respectively. RO-PV costs 2.99 $/m^3 while MVC-PV with the height cost of 3.97 $/m^3. Koroneos et al. [16] work was done only for a plant capacity of 500 m^3. Bourouni et al. [17] presented design models of five different configurations for two combinations which are PV-RO and Wind-RO. The authors did not include full economic study and comparison between the configurations. Furthermore, they based the power required on the minimum available renewable resources which result oversizing of the designed system. Several software tools were developed to simulate and optimize renewable energy systems [18,19]. The pur-

pose of these software tools is to estimate electrical production or heat generation or both. However, to the best of our knowledge, no published software tool has been developed to evaluate water production by renewable energy systems.

The selection of the appropriate method should go through a careful study of location and local circumstances [2,11]. Gude et al. [3] and Khan et al. [11] mentioned several parameters that affect the decision of the selection. These parameters include plant capacity, feed-water salinity, availability of grid, technical support and infrastructure, remoteness and local renewable resources. It is observed that most of the existing comparisons between different desalination technologies and specifically renewable powered desalination technologies were mainly based on various system capacity, energy source system, feed-water salinity, and system components. This makes the economic comparison almost impossible. There is an existing gap in having an economic comparison of different renewable powered desalination systems under the same conditions such as availability of renewable energy and water resources.

The objective of this research is to develop a systematic approach to determine the most cost-effective combination of renewable energy powered desalination system up to a certain extent. In this paper, we have focused on renewable energy powered RO systems. Though our work may be incomplete at this stage, the goal is to develop a systematic methodology and implement it in user-friendly software. In future stages, the methodology will be revised on a continuous basis, the cost models used for different components will be updated and improved. These updates and improvements will be applied to the software. In the near future, we expect that this software will be a useful tool to guide water government agencies or investors in this domain to help them choose the most effective technology for a given location. The focus of this research is the Gulf region of the Middle East (Saudi Arabia, UAE, Kuwait, and Qatar) which produce more than 40% of desalinated water worldwide and has vast renewable solar energy resources.

2. Selection methodology

To develop an optimum selection of renewable energy powered reverse osmosis desalination systems given the renewable energy and water resources of site geographical location the following methodology is followed:

- Based on water capacity needed and feed-water salinity, the energy needed to desalinate the required capacity of water is evaluated using reverse osmosis desalination system.
- Cost models are used to estimate installation, operation and maintenance and total costs based on the local prices for the geographical location considered.
- Using renewable energy data of the location considered, renewable power generation-systems sizes that are used to power the desalination systems are determined. Renewable energy generation systems include solar PV and wind turbine.
- Cost models are also used to estimate installation, operation and maintenance and total costs.
- Specific cost per cubic meter of distillate water is obtained for each renewable-desalination combination using the value of both systems.
- Specific costs for combinations are compared, and the combination that has the lowest specific cost is selected as the optimum renewable powered RO desalination system.

The above methodology is represented by a flowchart shown in Fig. 4.

The first step in implementing the methodology is to look at several renewable energy powered desalination systems. In order to limit our search space, we will only consider the most promising and practical combinations of renewable energy subsystem and desalination subsystem as discussed in the introduction.

Two combinations are presented here which are RO-Wind and RO-PV. Both of them following the same methodology except that in Wind-RO monthly average daily wind speed is used while in RO-PV a representative day in each month is selected and full-day simulation is used. Therefore, only the methodology of RO-wind is presented. Simple layouts of the RO-wind and RO-PV systems are presented in Figs. 5 and 6, respectively.

In order to come up with the appropriate design of wind-RO, the following methodology is applied. The presented methodology uses water storage to ensure water availability instead of energy storage. This selection makes the system more reliable, more economical, feasible espe-

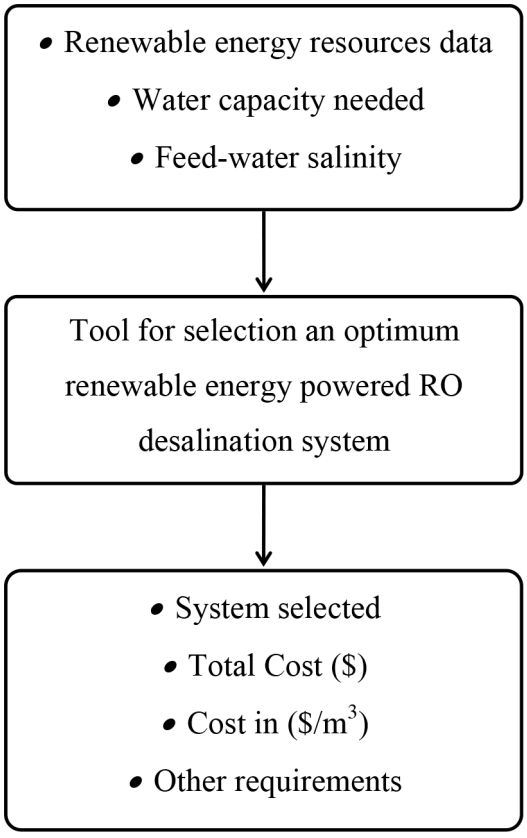

Fig. 4. Methodology flowchart.

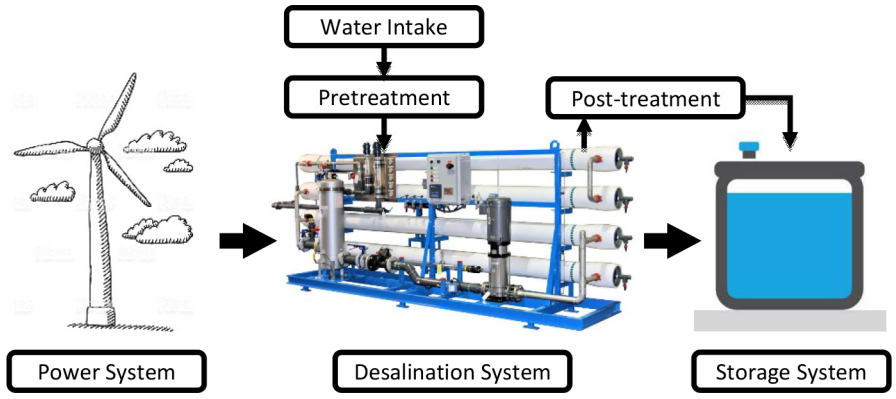

Fig. 5. Layout diagram of RO-Wind system.

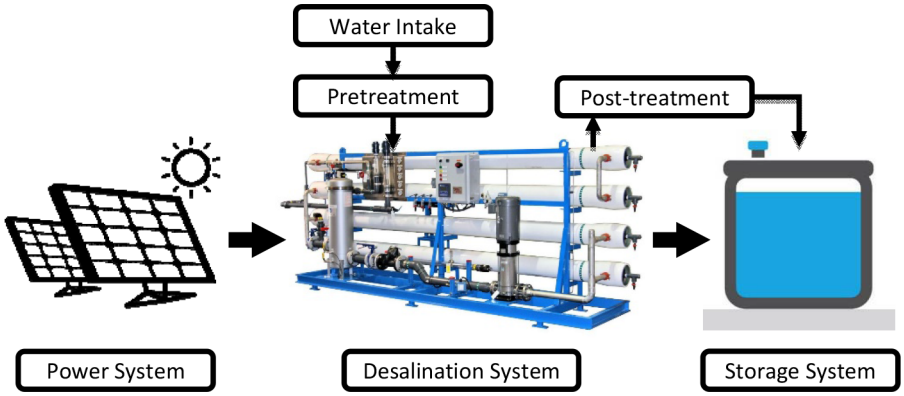

Fig. 6. Layout diagram of RO-PV system.

cially for large capacity, more environmentally friendly and it is in line with our primary goal of water production. The methodology is as the following:

- Based on water capacity needed ($M_{n,avg}$) and feed-water salinity, the size needed to desalinate the required capacity of water using reverse osmosis desalination system is evaluated. The size of the RO system is mainly determined by the number of pressure vessels ($N_{Pressurevessels}$).
- Once the size of the RO system is decided, the power required is evaluated then the number of wind turbines ($N_{Turbines}$) is determined using yearly average wind speed.
- Power produced by the wind farm in each month is evaluated ($P_{wind,i}$, $i = 1, 12$) based on actual weather data.
- Monthly and monthly average water production is evaluated ($M_{d,i}$, $i = 1, 12$ *and* $M_{d,avg}$) based on monthly power production.
- In some months, all energy produced is utilized to desalinate water. In others, the energy generated is more than the maximum power required by the desalination system, so some of the energy is excess. Excess of energy (EE) is evaluated.
- If average water production is less than average water demand and there is no excess of energy, this means the power system is not enough to produce the required water capacity, so we need to size up the power system by one additional turbine. If there is energy excess, we increase the size of the RO system by adding one pressure vessel.
- Finally, the storage tank status is evaluated at the end of each month ($Tank_i$, $i = 1, 12$) to ensure the availability of water. Size of the storage tank is determined by the maximum water volume available in the storage tank at the end of each month and the minimum storage size is determined by water demand for 30 days.
- The total and specific cost of power, desalination, and storage systems are evaluated.

The above-explained methodology for RO-Wind is depicted in Fig. 7.

As previously mentioned, the methodology followed in RO-PV is very similar to RO-Wind except in having full-day operation evaluation for an average day in each month.

It is important to recall that we use water storage instead of energy storage. For this purpose, the status of the tank is monitored for the first twelve months to guarantee water supply by the system in all months. Size of the container is determined by the maximum water storage volume required and the minimum storage tank size is determined by water demand for one month. Water production is not the same in all months.

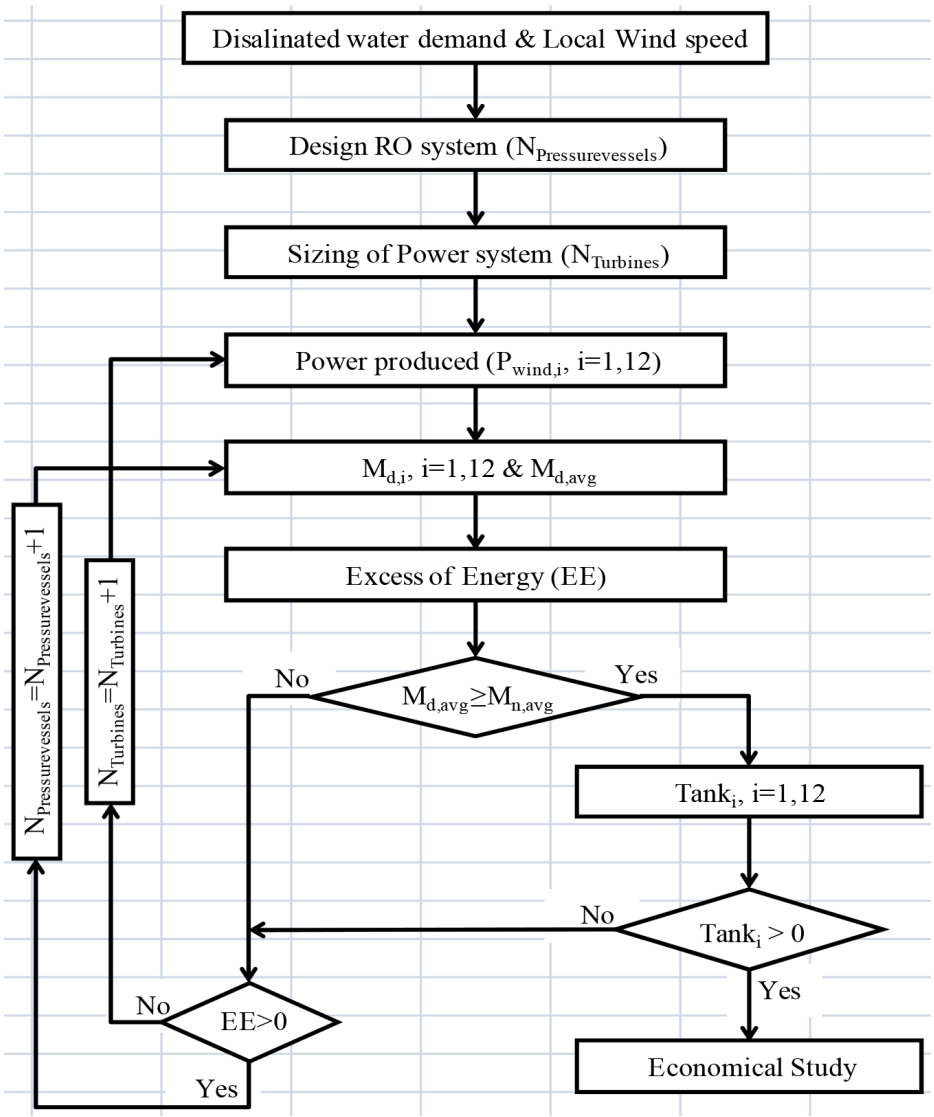

Fig. 7. Flowchart of the presented methodology for RO-Wind.

It is a function of renewable resources available and renewable power system size. So, water production in some months will be more than the needed to balance the months with lower renewable resources. Therefore, the status of the water storage tank is strongly dependent on the starting month.

To demonstrate the presented methodology, cases of both RO-wind and RO-PV are analyzed. The fixed parameters for which these cases are investigated are summarized in Table 1. The analysis is done for Dhahran, Saudi Arabia. Renewable resources for Dhahran including monthly average daily solar insolation (kWh/m^2/d), monthly average wind speed and monthly average mean temperature are shown in Table 2.

To apply the proposed methodology, thermodynamics and economic modeling of solar photovoltaic, wind and reverse osmosis are developed. These models are presented in the following section. Each model is validated against previous work.

Table 1
Fixed design parameters of RO-Wind and RO-PV cases

Quantity (unit)	Value
Daily water demand (m^3)	1,000
Feed water salt concentration (ppm)	45,000
Feed water temperature (°C)	25
Recovery ratio (%)	30
Membrane area (m^2)	35.4
Number of elements in each pressure vessel (–)	7

3. Mathematical modeling

3.1. Photovoltaic (PV) power modeling

The modeling of a PV array includes solar radiation modeling and PV power generation modeling. The solar radiation modeling estimates the radiation incident on a

Table 2
Monthly average weather data for Dhahran, Saudi Arabia [20]

Month	Insolation (kWh/m²/d)	Wind speed (m/s)	Mean temperature (°C)
January	3.348	5.95	14.4
February	4.377	5.70	16.8
March	5.181	5.50	20.9
April	6.257	4.80	25.5
May	6.970	5.40	31.6
June	7.870	6.60	35.8
July	7.344	4.90	37.3
August	6.965	4.70	36.6
September	6.343	4.30	33.2
October	5.249	4.90	30.3
November	4.091	6.05	23.6
December	3.336	6.00	19.0

Table 3
Average days of each month and number of the day in the year [21]

Month	Date	*n*
January	17	17
February	16	47
March	16	75
April	15	105
May	15	135
June	11	162
July	17	198
August	16	228
September	15	258
October	15	288
November	14	318
December	10	344

tilted surface. The PV generation model estimates the PV array output power based on the incident solar radiation, weather conditions, and PV panel specification.

In the present analysis, the incident solar radiation is evaluated for each hour on an average day of each month. The used model is obtained from [21]. Table 3 shows the average days of each month and their number of the day in the year, *n*. Radiation on a horizontal surface is obtained using the ratio of hourly, *I*, and daily, *H*, total radiation on the horizontal surface r_t expressed as Eqs. (1) and (2):

$$r_t = \frac{I}{H} \tag{1}$$

$$r_t = \frac{\pi}{24}(a + b\cos\omega)\left[\frac{\cos\omega - \cos\omega_s}{\sin\omega_s - \frac{\pi\omega_s}{180}\cos\omega_s}\right] \tag{2}$$

$$a = 0.409 + 0.5016\sin(\omega_s - 60)$$

$$b = 0.6609 - 0.4767\sin(\omega_s - 60)$$

where ω is the hour angle in degrees and ω_s is the sunset hour angle which could be found by Eq. (3):

$$\cos\omega_s = -\tan\phi\tan\delta \tag{3}$$

where ϕ is the latitude and δ is the declination angle of the sun and could be approximated by Cooper's equation "1969" (4):

$$\delta = 23.45\sin\left(360\left(\frac{284+n}{365}\right)\right) \tag{4}$$

Total radiation on the tilted surface based on the isotropic diffuse model is composed of three main components: beam, diffuse, and reflected and it is evaluated by Eq. (5):

$$I_T = I_b R_b + I_d\left(\frac{1+\cos\beta}{2}\right) + I\rho_g\left(\frac{1-\cos\beta}{2}\right) \tag{5}$$

To evaluate I_b and I_d, Erbs et al. suggested correlation (6):

$$\frac{I_d}{I} = \begin{cases} 1.0 - 0.09k_T \ for\ k_T \le 0.22 \\ 0.9511 - 0.1604k_T + 4.388k_T^2 - 16.638k_T^3 \\ \quad + 12.336k_T^4 \ for\ 0.22 < k_T \le 0.8 \\ 0.165 \ for\ k_T \le 0.8 \end{cases} \tag{6}$$

where k_T is hourly clearness index and it is defined as $k_T = I/I_o$.

I_o is the extraterrestrial radiation on a horizontal surface for an hour period of time bounded by hour angles ω_2 and ω_1 where ω_2 is larger. Extraterrestrial radiation could be found by Eq. (7):

$$I_o = \frac{12\times 3600}{\pi} G_{sc} \times \left(1 + 0.033\cos\left(\frac{360n}{365}\right)\right) \times \left[\begin{array}{l} \cos\phi\cos\delta(\sin\omega_2 - \sin\omega_1) + \\ \left(\frac{\pi(\omega_2 - \omega_1)}{180}\right)\sin\phi\sin\delta \end{array}\right] \tag{7}$$

G_{sc} is solar constant and it is equal to 1367 W/m² or 4.92 MJ/m²·h.

Now, diffuse and beam radiation are evaluated by Eq. (8):

$$I_d = \left(\frac{I_d}{I}\right) \times I \ and \ I_b = \left(1 - \frac{I_d}{I}\right) I \tag{8}$$

The ratio of beam radiation on the tilted surface to that on the horizontal surface (R_b) is defined for the northern hemisphere as Eq. (9):

$$R_b = \frac{\cos(\phi - \beta)\cos\delta\cos\omega + \sin(\phi - \beta)\sin\delta}{\cos\phi\cos\delta\cos\omega + \sin\phi\sin\delta} \tag{9}$$

where β is the slope of the tilted surface.

ρ_g is ground reflectance and it is taken as 0.2 for Dhahran, Saudi Arabia [15].

These equations represent complete modeling to find total solar radiation of a tilted surface. PV power generation can be obtained by the model presented in [15]. PV power generation is a strong function of solar radiation and cell temperature. Cell temperature (T_c) can be found by Eq. (10):

$$T_c = T_a + I_T\left(1-\frac{\eta_c}{\tau\alpha}\right)\left(\frac{\tau\alpha}{U_L}\right) \tag{10}$$

where T_a is ambient temperature, η_c is electrical conversion efficiency, τ is solar transmittance of PV module, α is the solar absorption of the module and U_L is the overall loss coefficient. The quantity $\tau\alpha/U_L$ could be estimated by Eq. (11):

$$\frac{\tau\alpha}{U_L} = \frac{T_{C,NOCT} - T_{a,NOCT}}{I_{T,NOCT}} \tag{11}$$

$T_{C,NOCT}$ is normal operating cell temperature (NOCT) which is defined as the cell temperature at no load operation (η_c = 0), an incident radiation ($I_{T,NOCT}$) of 800 W/m^2, an ambient temperature ($T_{a,NOCT}$) of 20°C with an average wind speed of 1 m/s.

Cell efficiency η_c is assumed to be equal to maximum power point efficiency (η_{mp}) and it is equal to (12):

$$\eta_c = \eta_{mp} = \eta_{mp,std}\left[1+\alpha_p\left(T_c - T_{c,std}\right)\right] \tag{12}$$

where $\eta_{mp,std}$ is the maximum efficiency under the standard reference conditions which include the radiation flux ($I_{T,stc}$) of 1000 W/m^2, the PV cell temperature ($T_{c,std}$) of 25°C, air mass ratio of 1.5 and zero wind speed. α_p is temperature degradation coefficient [15].

PV output power could be calculated by Eq. (13):

$$P_{mp} = P_{mp,std}\left(\frac{I_T}{I_{T,stc}}\right)\left[1+\alpha_p\left(T_c - T_{c,std}\right)\right] \tag{13}$$

where $P_{mp,std}$ is cell maximum power at standard reference conditions.

The presented PV power generation model was implemented in the engineering equation solver (EES) software package. The developed model is validated against the results presented in [15]. Technical data for the PV module is shown in Table 4.

Table 4
Technical data of PV module

Model	Megasol solar panel
Rated power	185 W
Area	1.46 m × 0.66 m
η_MPPT	92%
Power temperature coefficient	–0.38% /K
Cost	290 $
Lifetime	20 years
Operation cost	2% of total capital cost
Packing factor	0.75

3.2. Wind power modeling

Wind power is one of the most important renewable power systems. In this section, a mathematical model of the wind turbine is presented. The dominant parameter that affects the wind turbine output is wind speed. When evaluating the power output from a wind turbine, wind speed has to be calculated at the turbine elevation. Eq. (14) is used where υ and υ_o are wind speeds at hub height z and reference height z_o, respectively. α is the ground surface friction coefficient and typically taken as (1/7) [22].

$$\frac{v}{v_o} = \left(\frac{z}{z_o}\right)^{\alpha} \tag{14}$$

Wind turbine power output is usually evaluated using its characteristic curve. For programming purposes, curve fitting is used for the evaluation. To guarantee the best fitting, several polynomials as shown in Eq. (15) are used.

$$P_W(v) = \begin{cases} 0,\ for\ v < v_c \\ a_1 v^n \ldots . b_1 v^2 + c_1 v + d_1, v_c \le for\ \ v < v_1 \\ a_2 v^n \ldots . b_2 v^2 + c_2 v + d_2, v_1 \le for\ \ v < v_2 \\ a_3 v^n \ldots . b_3 v^2 + c_3 v + d_3, v_2 \le for\ \ v < v_3 \\ 0,\ for\ \ v > v_f \end{cases} \tag{15}$$

where υ_c and υ_f are the cut-in and cut-off wind speed of the wind turbine.

Presented wind turbine model is validated with [23]. In the presented analysis, the horizontal axis wind turbine Nordex N27/15 is used. Technical data for the turbine is shown in Table 5 [23].

3.3. Reverse osmosis modeling

The mathematical thermodynamics model of RO system is developed as presented in [24].

Recovery ratio is the ratio of distillate mass flow rate to feed mass flow rate:

$$\text{Recovery Ratio} = \frac{\text{M}_{\text{distillate}}}{\text{M}_{\text{feed}}} \tag{16}$$

Salt rejection percentage:

$$\text{Salt Rejection} = \frac{X_{\text{feed}} - X_{\text{distillate}}}{X_{\text{feed}}} \tag{17}$$

where X is salt concentration.

Table 5
Technical data of the wind turbine

Model	Nordex N27/15
Rated power	150 kW
Rated speed	16.0 m/s
Cut-in speed (VC)	3–4 m/s
Cut-out speed (Vf)	25 m/s
Capital cost	150,000 $
Lifetime	20 years
Operation cost	2% of total capital cost

Mass conservation equation:

$$\mathrm{M}_{\mathrm{feed}} = \mathrm{M}_{\mathrm{distillate}} + \mathrm{M}_{\mathrm{brine}} \tag{18}$$

Salt mass conservation equation:

$$\mathrm{M}_{\mathrm{feed}} \times X_{\mathrm{feed}} = \mathrm{M}_{\mathrm{distillate}} \times X_{\mathrm{distillate}} + \mathrm{M}_{\mathrm{brine}} \times X_{\mathrm{brine}} \tag{19}$$

Average salt concentration $\overline{X}$ is equal to:

$$\overline{X} = \frac{\mathrm{M}_{\mathrm{feed}} \times X_{\mathrm{feed}} + \mathrm{M}_{\mathrm{brine}} \times X_{\mathrm{brine}}}{\mathrm{M}_{\mathrm{feed}} + \mathrm{M}_{\mathrm{brine}}} \tag{20}$$

Distillate water salt concentration could be found by Eq. (21):

$$X_{\mathrm{distillate}} = \frac{\mathrm{M}_{\mathrm{salt}}}{\mathrm{M}_{\mathrm{distillate}}} \tag{21}$$

where M_{salt} for each membrane is evaluated by Eq. (22):

$$\mathrm{M}_{\mathrm{salt}} = \left(\overline{X} - X_{\mathrm{distillate}}\right) k_S A \tag{22}$$

Temperature correction factor TCF equation:

$$TCF = \exp\left[2700 \times \left(\frac{1}{T+273} + \frac{1}{298}\right)\right] \tag{23}$$

where T is the feed water temperature.

Membrane water permeability k_w:

$$k_w = 6.84 \times 10^{-8} \times \frac{18.6865 - \left(0.177 \times X_{\mathrm{brine}}\right)}{T+273} \tag{24}$$

Membrane salt permeability k_S:

$$k_S = FF \times TCF \times 4.72 \times 10^{-7} \times \left[0.06201 - \left(5.31 \times 10^{-5} \times (T+273)\right)\right] \tag{25}$$

where FF is the fouling factor, and it is equal to one for a new membrane.

An approximation for osmotic pressure is obtained by assuming 1000 ppm of total dissolved solids (TDS) equals to 75.84 kPa of osmotic pressure. So osmotic pressure is equal to:

$$\Pi = 75.84 \times X \text{ for feed, distillate and brine} \tag{26}$$

Average osmotic pressure:

$$\Pi_{avg} = 0.5 \times \left(\Pi_{feed} + \Pi_{brine}\right) \tag{27}$$

Net osmotic pressure:

$$\Delta\Pi = \Pi_{avg} - \Pi_{distillate} \tag{28}$$

Net pressure difference:

$$\Delta P = \left(\frac{\mathrm{M}_{\mathrm{distillate}}}{TCF \times FF \times A \times n_e \times n_v \times k_W}\right) + \Delta\Pi \tag{29}$$

where A is element area; n_v is the number of pressure vessels; n_e is the number of elements in each pressure vessel.

Power required for RO driving pump in (kW) is evaluated by Eq. (30):

$$HP = \left(\frac{\mathrm{M}_{\mathrm{distillate}} \times \Delta P}{\eta_{pump}}\right) \tag{30}$$

Specific power consumption:

$$SPC = \frac{HP}{\mathrm{M}_{distillate}} \tag{31}$$

Using the engineering equation solver (EES) packages, RO mathematical model [Eqs. (16)–(31)] is implemented. Results are validated against the results presented in [25]. Table 6 shows the results obtained using the developed model and results obtained in different models used in [25]. In the analysis, the membrane SW30HR-380 is used. The technical data of the membrane is given in Table 7 [26].

Cost evaluation for reverse osmosis plant is obtained by the model presented in [25]. Total cost is mainly based on two components; capital, and operation and maintenance costs. Total capital cost (TCC) is the summation of direct (DCC) and indirect (ICC) capital costs as expressed in Eq. (32):

$$TCC = DCC + ICC \tag{32}$$

where direct capital cost (DCC) is composed of:

$$DCC = CC_{equip} + CC_{site} \tag{33}$$

Table 6
Validation of RO mathematical model

Parameter	Model used in this study	Model used in [25]	VDS	ROSA6.1
			As presented in [25]	
SPC, kWh/m^3	7.921	7.68	7.76	7.76
HP, kW	1155	1131	1130	1131.42
M_f, M^3/h	486	485.9	486	458.9
M_b, M^3/h	340.2	340.1	340.23	340.15
X_b, ppm	64,179	64,180	66,670	62,005
X_d, ppm	250	250	200	283.83
SR	0.9944	0.9944	0.9927	–
ΔP, kPa	6843	6850	6700	6670

Table 7
Technical data of RO membrane [26]

Model	SW30HR-380
Active area (m^2)	35.3
Feed flow rate range (m^3/h)	0.8–16
Permeate flow (m^3/d)	22.7
Cost of RO element ($)	1000
Cost of pressure vessel ($)	1000

Equipment capital cost (CC_{equip}) is mainly divided into:

$$CC_{equip} = CC_{swip} + CC_{hpp} + CC_e \quad (34)$$

Seawater intake and pretreatment (CC_{swip}) and a high pressure pump (CC_{hpp}) capital costs are evaluated as presented in [27]:

$$CC_{swip} = 996 \times M_{feed}^{0.8} \quad (35)$$

$$CC_{hpp} = 393{,}000 + 10{,}710 \times \Delta P_f \text{ where } \Delta P_f \text{ is feed pressure} \quad (36)$$

Elements capital cost (CC_e) is evaluated by Eq. (37):

$$CC_e = P_P \times n_e \times n_v + PV_P \times n_v \quad (37)$$

where P_p and PV_p are unit costs of membrane elements and pressure vessels, respectively.

Site capital cost (CC_{site}) is estimated to be 10% of equipment capital cost (CC_{equip}). Also, Indirect capital cost (ICC) is estimated as 27% of the direct capital cost (DCC). Total capital cost (TCC) is the summation of direct and indirect capital costs.

Annual capital cost (ACC) is evaluated by Eq. (38):

$$ACC = TCC \times A_f \quad (38)$$

where A_f is called the amortization factor and it is found by Eq. (39):

$$A_f = \frac{i(1+i)^{LT_P}}{(1+i)^{LT_P} - 1} \quad (39)$$

where i is the interest rate and it is equal to 5%. LT_p is the life time of the project and it is equal to 20 years.

Total operational cost (OC_{Total}) is composed of power (OC_{Power}), labor (OC_{Labor}), chemicals (OC_{chm}), insurance (OC_{insur}), and membrane (OC_{memb}) operational costs. Each of them is evaluated as Eqs. (40)–(44):

$$OC_{Power} = LF \times 0.06 \times SPC \times M_{distillate} \quad (40)$$

$$OC_{Labor} = LF \times 0.01 \times M_{distillate} \quad (41)$$

$$OC_{chm} = LF \times 0.04 \times M_{distillate} \quad (42)$$

$$OC_{insur} = 0.005 \times TCC \times M_{distillate} \quad (43)$$

$$OC_{memb} = P_P \times n_e \times \frac{n_v}{LT_m} \quad (44)$$

where LF is the load factor of the plant, and it is equal to 0.9, LT_m is the life time of the membrane and it is equal to 5 years. Hourly cost of the RO plant ($/h) is equal to:

$$Z_{RO} = \frac{(ACC + OC_{Total})}{8760} \quad (45)$$

Evaluating RO specific cost of water ($/m^3) can be done now by dividing the hourly value by hourly water production:

$$C_{RO} = \frac{Z_{RO}}{M_{distillate}} \quad (46)$$

In addition to power and desalination systems, a storage system is needed. The methodology applies the water storage instead of the energy storage because it is harmonized with the primary goal of water production. Also, it is a more cost-effective choice and environmentally-friendly. The features of the storage system are shown in Table 8.

Table 8
Features of water storage system

Feature	#
Capacity of one tank (m^3)	10,000
Cost of one tank ($)	300500
Lifetime (y)	50
Interest rate (%)	5

4. Results and discussion

The presented methodology of RO-PV and RO-Wind including thermo-economic models of solar photovoltaic, wind and reverse osmosis are implemented in engineering equation solver (EES) software package. EES is an equation solver used to find the numerical solution of non-linear algebraic equations. The equations could be broken down into subprograms, functions, and procedures. The equations of the main program and each sub-program are solved simultaneously. EES automatically recognizes and groups equations that should be solved simultaneously. If specific equations order to be followed, then functions or procedures should be used.

To illustrate the application of the methodology, different cases for RO-wind and RO-PV are analyzed and compared for the city of Dhahran, Saudi Arabia. For RO-wind, six different cases are presented in Table 9 to show different scenarios. The first four cases have the same power system size and desalination system size. Therefore, average water production in each month is the same for these cases as shown in Fig. 8. They differ only in the operation-starting-month. Although the methodology introduced guarantees that average water production is more than water demand, the status of the storage tank should be considered to also guarantees a continuous supply of desalinated water, especially in the first years. Fig. 9 shows the status of the storage tank at the end of each month for the six cases. Status of the water tank is strongly dependent of the starting month and therefore it should be carefully considered, otherwise larger desalination system – and may be power system – will be needed to satisfy the continuous supply of water. Beginning the desalination process from January (Case 1) is good enough in this case since water is available throughout the year. January is a good month to start with since its average wind speed is higher than the yearly average wind speed and it is followed by months of also higher wind speed than the average i.e. February and March. This helps water to accumulate in the tank to be used in months with lower wind speed and lower water production as a

Table 9
Six different cases of RO-wind for Dhahran, Saudi Arabia (wind speed data is given in Table 2 above)

	Case 1	Case 2	Case 3	Case 4	Case 5	Case 6
Daily water demand (m^3)			1,000			
Daily average water production (m^3)	1,027	1,027	1,027	1,027	1,090	1,148
Starting month	January	February	June	November	February	June
No. of turbines	6	6	6	6	6	6
No. of pressure vessels	10	10	10	10	11	12
No. of storage tanks	3	3	3	3	4	6
Water specific cost ($/$m^3$) (based on water production)	1.366	1.366	1.366	1.366	1.395	1.471

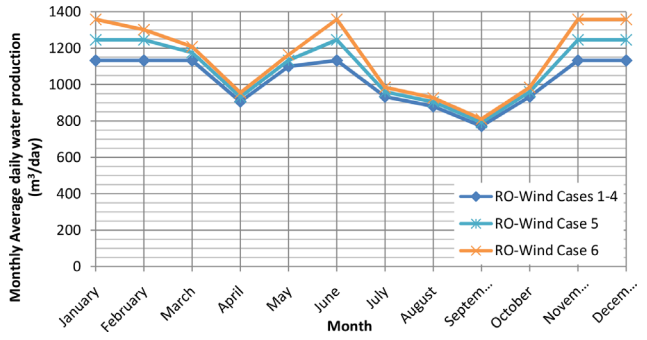

Fig. 8. Monthly average daily water production for six cases of RO-wind.

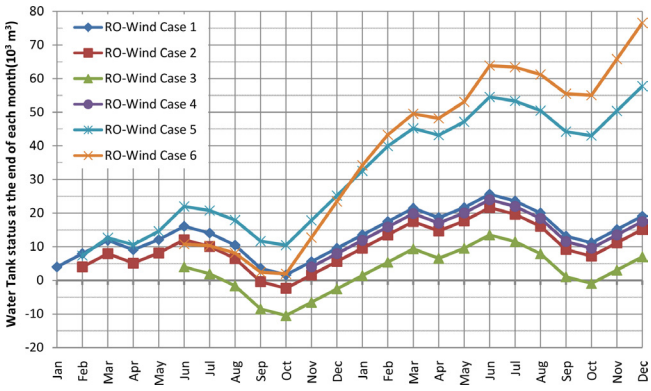

Fig. 9. Water tank status at the end of each month for six cases of RO-wind.

result. Status of the tank for the first year for Case 1 can be seen in Fig. 9.

Starting the operation in February (Case 2) is not a preferred choice because we will reach a point where water demand is more than water available in September and October. To overcome this issue, the code will size up the RO plant by one additional pressure vessel. This will result in increasing average water production as seen in Figs. 8 and 9 for Case 5. Thus, the number of storage tanks is increased. Specific cost based on water production is reduced because no additional wind turbines are needed, so the reduction in the specific cost of the power system is more than the increment in specific cost of desalination and storage systems.

Starting the operation in June (Case 3) seems to be attractive since it has the maximum wind speed but because it is followed by four months of lower wind speed – lower than the average – which will result in running out of the water. In fact, June is one of the worst months in starting the operation, and two pressure vessels are required to satisfy the demand. Case 6 in Figs. 8 and 9 is representing the modification of Case 2.

Case 4 is representing the starting operation in November. It is observed that water is available in storage tanks throughout the year. It can be approved that for Dhahran, November is the best month to start the operation because it is the first month in consecutive months of wind speed higher than the average, i.e., December, January, February, and March.

In applying the proposed methodology, selection of the starting month is important and it should go through careful study. It is location property, and November is the best month for Dhahran. Therefore, November is selected to be the starting month of wind power systems throughout this study.

Sometimes the concept of sizing up the desalination system, or power system, or both is not a practical solution. Therefore, we could look at it from another point of view which is how long the period required to reach steady state water availability where water will be available in the storage tanks throughout the year. The required period is expressed in years and depend strongly on the operation starting month. The case of RO-PV is presented in Table 10. The period required to reach steady state water availability for different cases of operation starting month is shown in Table 11. The table shows that if the operation begins in January, the steady-state water availability will only be reached by the third year. During the first two years, additional water source should be used to guarantee continuous water supply to the community. The steady-state water availability will be obtained from the first year if the operation starts from April since it is the first month in consecutive months where monthly average daily radiation is higher than yearly average daily radiation – having global radiation more than the average means producing desalinated water more than the demand. Therefore, April is selected to be the starting month for solar PV throughout this study.

Cost of water by wind is less than the cost of water by solar. For daily average water demand of 1,000 m^3, cost of water in RO-wind (Case 4) is 1.366 $/$m^3$ while in RO-PV

Table 10
Results of the case of RO-PV for Dhahran, Saudi Arabia (solar data is given in Table 2)

Quantity	#
Daily water demand (m^3)	1,000
Daily average water production (m^3)	1,016
No. of PV panels	8,778
No. of pressure vessels	27
No. of storage tanks	3
Water specific cost ($/m^3$) (based on water production)	2.119

Table 11
Steady-state water availability period required for different cases of operation starting month of RO-PV

Operation starting month	Steady-state water availability reached by:
January	Third year
April	First year
June	Second year
November	Fourth year

it is 2.119 $/m^3$. This difference is not only because of the difference in costs of power systems but also because of the larger desalination system needed in solar. Larger system – number of pressure vessels is 10 in the wind while it is 27 in PV – is necessary to overcome a long time of no water production during the night. This increment in size is considered as a replacement for energy storage.

Previous analysis was obtained under fixed feed water concentration of 45,000 ppm. A similar methodology is applied to different feed water concentration. Fig. 10 shows the specific cost of water produced by RO-wind and RO-PV at feed water concentration ranging from 25,000 ppm to 60,000 ppm where the average water demand is fixed as 1,000 m^3/d. It is observed that the cost is increased exponentially in both combinations as the feed water concentration increased. Also, as noted, the difference between the cost of water by RO-PV and cost of water by RO-Wind is increasing from 0.52 $/m^3$ for 25,000 ppm to 1.019 $/m^3$ for 60,000 ppm.

It is essential to study water cost at different system sizes. Based on the concept of scale, the price is expected to decrease as the size increases. Fig. 11 presents water cost at different daily average water demand using both techniques, RO-wind and RO-PV. As expected, the cost is decreasing as the capacity increases. The difference in cost between RO-PV and RO-wind is almost 0.72 $/m^3$ for all cases. As explained, the larger RO plant required in PV is mainly the reason behind this difference. As seen in Figs. 12 and 13, the number of storage tanks is the same for both combinations while the number of pressure vessels in PV is 2.5 multiple pressure vessels in wind.

It is crucial to consider the safety factor in the design of desalination plants. The importance of safety factor is to overcome any sudden reduction in water availability caused by sudden or planned shutdown of the plant or

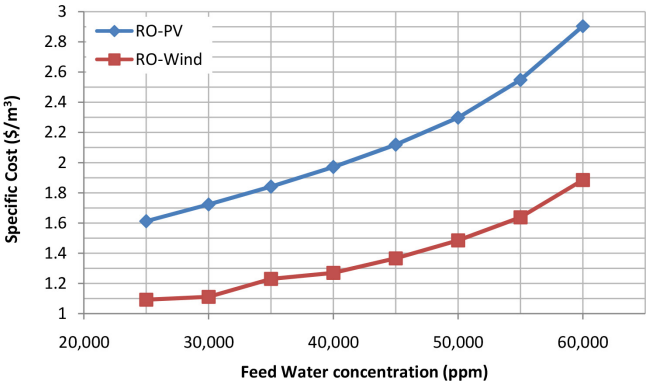

Fig. 10. Water cost for system daily capacity of 1,000 m^3 using RO-Wind and RO-PV at different feed water concentration.

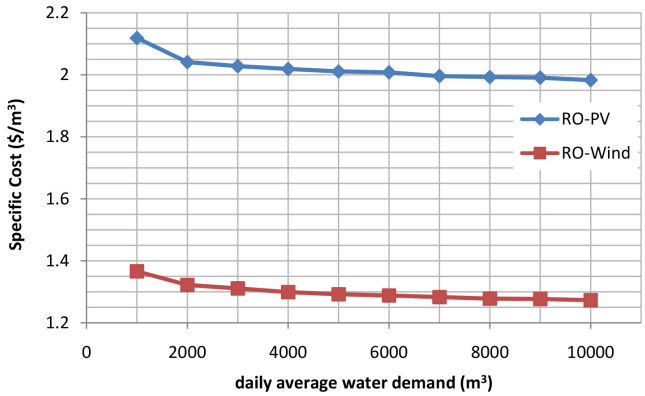

Fig. 11. Cost of water produced by RO-wind and RO-PV at different water demand capacity.

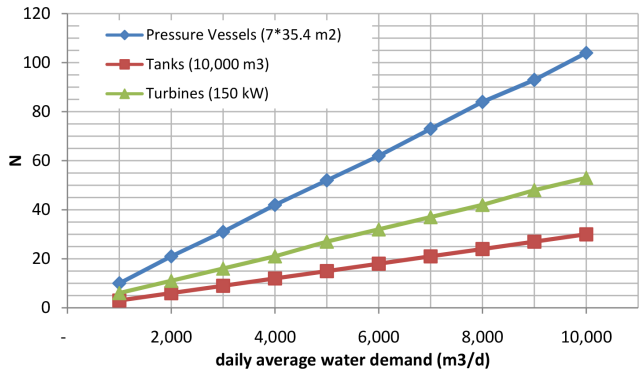

Fig. 12. Number of pressure vessels, storage tanks and wind turbines used at different system capacity.

due to drastic weather changes. Safety factor in this study is expressed as a percentage of water demand. The system size is determined based on the overall water demand including the additional amount considered as a safety factor. Fig. 14 shows the cost of water for a plant capacity of 10,000 m^3/d for the two systems of RO-wind and RO-PV. Cost of water reduces slightly as the safety factor increases. For RO-wind, the cost reduces from 1.273 $/m^3$ for the primary system with zero safety factor to

1.262 $/m^3 for the system with 50% safety factor. Similar behavior is observed for RO-PV.

An easy-to-use interface window is developed using an embedded tool in EES. The window simplifies the usage of the code. The interface shows the inputs, which are daily water demand, feed water concentration, and safety factor, and outputs, which are the specific cost of each combination and the combination with the minimum cost. Fig. 15 shows the interface window. The case shown is the same case discussed above.

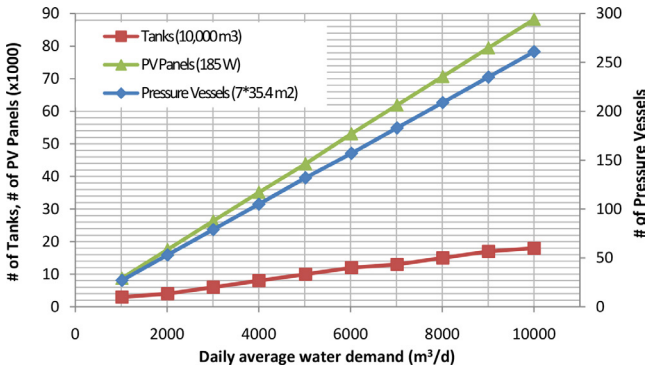

Fig. 13. Number of pressure vessels, storage tanks and PV panels used at different system capacity.

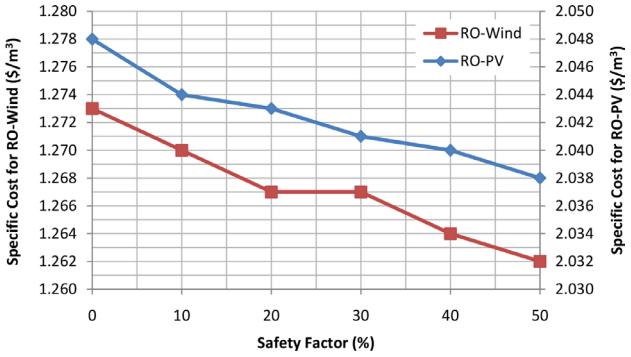

Fig. 14. specific cost of water at different safety factors for a system capacity of 10,000 m^3/d.

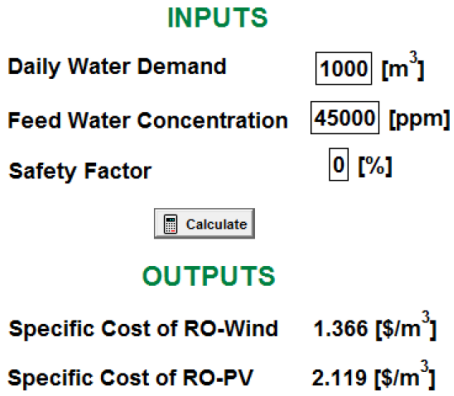

Fig. 15. Developed interface window in EES.

5. Conclusion

We have presented a thermo-economic methodology for selecting the most economical renewable energy powered reverse osmosis desalination system given a geographical location, based on the weather data and required freshwater demand. The methodology has been formulated based on the common published models of renewable energy and RO desalination subsystems. In order to facilitate the use of this methodology, we have implemented it in EES software and used the code to simulate several practical cases.

For the case of Dhahran, Saudi Arabia, the method predicted that an RO-wind system produced desalinated water at the cost of \$1.366/m^3 for a daily demand of 1,000 m^3. This cost was in favor of an RO-PV system with a cost of \$2.119/m^3.

Our implementation uses water storage as a method to ensure the availability of water at any time. This choice, we think, is more cost-effective, more environmentally friendly and in line with our primary goal of water production, if compared to energy storage using batteries. The method will be generalized for more renewable-energy-desalination practical combinations.

Acknowledgment

The authors would like to acknowledge the support of King Fahd University of Petroleum and Minerals during this research investigation.

Symbols

EE — Energy excess
N — Number of
P — Power
REDS — Renewable energy desalination systems
Tank — Water volume in the storage tank

Subscripts

avg — average
d — distillate
i — number of the month
n — needed

The Optimum Renewable Energy
Powered Desalination System is
Wind Energy Powered Reverse Osmosis
with specific water production cost of
1.366 [$/m^3]

References

[1] International Desalination Association, Desalination by the Numbers | IDA, HIDE & SEEK MEDIA, 30 June 2015. [Online]. Available: http://idadesal.org/desalination-101/desalination-by-the-numbers/. [Accessed 8 May 2018].

[2] A. Al-Karaghouli, D. Renne, L.L. Kazmerski, Solar and wind opportunities for water desalination in the Arab regions, Renew. Sustain. Energy Rev., 13 (2009) 2397–2407.

[3] V.G. Gude, N. Nirmalakhandan, S. Deng, Renewable and sustainable approaches for desalination, Renew. Sustain. Energy Rev., 14 (2010) 2641–2654.

[4] N. Ghaffour, J. Bundschuh, H. Mahmoudi, M.F. Goosen, Renewable energy-driven desalination technologies: A comprehensive review on challenges and potential applications of integrated systems, Desalination, 356 (2015) 94–114.

[5] S.A. Kalogirou, Seawater desalination using renewable energy sources, Progr. Energy Combust. Sci., 31 (2005) 242–281.

[6] A. Chauhan, R. Saini, A review on integrated renewable energy system based power generation for stand-alone applications: Configurations, storage options, sizing methodologies and control, Renew. Sustain. Energy Rev., 38 (2014) 99–120.

[7] M.T. Ali, H.E. Fath, P.R. Armstrong, A comprehensive techno-economical review of indirect solar desalination, Renew. Sustain. Energy Rev., 15 (2011) 4187–4199.

[8] M.A. Eltawil, Z. Zhengming, L. Yuan, A review of renewable energy technologies integrated with desalination systems, Renew. Sustain. Energy Rev., 13 (2009) 2245–2262.

[9] Q. Ma, H. Lu, Wind energy technologies integrated with desalination systems: Review and state-of-the-art, Desalination, 277 (2011) 274–280.

[10] I.C. Karagiannis, P.G. Soldatos, Water desalination cost literature: review and assessment, Desalination, 223 (2008) 448–456.

[11] M.A. Khan, S. Rehman, F.A. Al-Sulaiman, A hybrid renewable energy system as a potential energy source for water desalination using reverse osmosis: A review, Renew. Sustain. Energy Rev., 97 (2018) 456–477.

[12] A. Al-Karaghouli, L.L. Kazmerski, Energy consumption and water production cost of conventional and renewable-energy-powered desalination processes, Renew. Sustain. Energy Rev., 24 (2013) 343–356.

[13] J. Rheinländer, E.W. Perz, O. Goebel, Performance simulation of integrated water and power systems — software tools IPSEpro and RESYSpro for technical, economic and ecological analysis, Desalination, 157 (2003) 57–64.

[14] E.W. Perz, S. Bergmann, A simulation environment for the techno-economic performance prediction of water and power cogeneration systems using renewable and fossil energy sources, Desalination, 203 (2007) 337–345.

[15] N. Ahmad, A.K. Sheikh, P. Gandhidasan, M. Elshafie, Modeling, simulation and performance evaluation of a community scale PVRO water desalination system operated by fixed and tracking PV panels: A case study for Dhahran city, Saudi Arabia, Renew. Energy, 75 (2015) 433–447.

[16] C. Koroneos, A. Dompros, G. Roumbas, Renewable energy driven desalination systems modelling, J. Cleaner Prod., 15 (2007) 449–464.

[17] K. Bourouni, T.B. M'Barek, A.A. Taee, Design and optimization of desalination reverse osmosis plants driven by renewable energies using genetic algorithms, Renew. Energy, 36 (2011) 936–950.

[18] S. Sinha, S. Chandel, Review of software tools for hybrid renewable energy systems, Renew. Sustain. Energy Rev., 32 (2014) 192–205.

[19] O. Erdinc, M. Uzunoglu, Optimum design of hybrid renewable energy systems: Overview of different approaches, Renew. Sustain. Energy Rev., 16 (2012) 1412–1425.

[20] M. Habib, S. Said, M. El-Hadidy, I. Al-Zaharna, Optimization procedure of a hybrid photo voltaic wind energy system, Energy, 24 (1999) 919–929.

[21] J. Duffie, W. Beckman, Solar Engineering of Thermal Processes, John Wiley and Sons, 2006.

[22] E.M. Mokheimer, A.Z. Sahin, A. Al-Sharafi, A.I. Ali, Modeling and optimization of hybrid wind–solar-powered reverse osmosis water desalination system in Saudi Arabia, Energy Convers. Manage., 75 (2013) 86–97.

[23] M. Elhadidy, S. Shaahid, Decentralized/stand-alone hybrid Wind–Diesel power systems to meet residential loads of hot coastal regions, Energy Convers. Manage., 46 (2005) 2501–2513.

[24] H.T. El-Dessouky, H.M. Ettouney, Fundamentals of Salt Water Desalination, Elsevier, 2002.

[25] A. Nafey, M. Sharaf, Combined solar organic rankine cycle with reverse osmosis desalination process: Energy, exergy, and cost evaluations, Renew. Energy, 35 (2010) 2571–2580.

[26] Y.-Y. Lu, Y.-D. Hu, X.-L. Zhang, L.-Y. Wu, Q.-Z. Liu, Optimum design of reverse osmosis system under different feed concentration and product specification, J. Membr. Sci., 287 (2007) 219–229.

[27] A. Malek, M. Hawlader, J. Ho, Design and economics of RO seawater desalination, Desalination, 105 (1996) 245–261.